Desalination and Water Treatment
www.deswater.com
49 (2012) 41–56
November
1944-3994/1944-3986
doi: 10.1080/19443994.2012.708197
Taylor & Francis
Taylor & Francis Group

Investigations on the batch performance of cationic dyes adsorption by citric acid modified peanut husk

Weihua Zou[a,*], Hongjuan Bai[a], Shuaipeng Gao[a], Xue Zhao[a], Runping Han[b,*]

[a]*School of Chemical Engineering and Energy, Zhengzhou University, 100# of Kexue Road, Zhengzhou 450001, P.R. China*
Tel./Fax: +86 371 67781801; email: whzou@zzu.edu.cn
[b]*Department of Chemistry, Zhengzhou University, 100# of Kexue Road, Zhengzhou 450001, P.R. China*
Email: rphan67@zzu.edu.cn

Received 4 January 2011; Accepted 3 June 2012

ABSTRACT

A citric acid modified peanut husk (MPH) was used as adsorbent for removal of neutral red (NR) and methylene blue (MB) from aqueous solution. A batch system was applied to study the behavior of NR and MB adsorption in single and binary systems on MPH. Such studies were conducted by varying various parameters such as the initial dye concentration, the pH, the salt concentration, the temperature, and the contact time. Adsorption kinetic data were fitted using pseudo-first-order equation, pseudo-second-order equation, and intraparticle diffusion model. The process mechanism was found to be complex, consisting of both surface adsorption and pore diffusion. The effective diffusion parameter D_i values estimated in the order of 10^{-8} cm^2/s indicated that the intraparticle diffusion was not the rate-controlling step. The NR adsorption isotherm follows the Langmuir model, while MB adsorption follows the Freundlich isotherm. The thermodynamics parameters of adsorption systems indicated spontaneous and endothermic process. In binary system, NR and MB exhibited competitive adsorption. The adsorption of NR or MB is considerably reduced with an increasing concentration of the other. The quantity of MB adsorbed is more strongly by NR due to the higher affinity of MPH for the latter.

Keywords: Modified peanut husk (MPH); Neutral red (NR); Methylene blue (MB); Adsorption; Mechanism

1. Introduction

Dyes usually have a synthetic origin and complex aromatic molecular structures which make them more stable and more difficult to biodegrade. Dyes are important pollutants, causing environmental and health problems to human beings and aquatic animals [1]. So, it is necessary for the colored effluents to be treated properly before they are discharged into the water bodies [2]. Removal of dyes from wastewater can be achieved by several techniques, such as reverse osmosis, electrodialysis, ultrafiltration, ion exchange, chemical precipitation, etc. [3]. However, all these methods may suffer from one or more limitations and are not successful in completely removing the dyestuff from wastewater [4]. In contrast, adsorption has emerged as an efficient and cost-effective alternative to conventional contaminated water treatment facilities. The most widely used adsorbent for the removal of dyes is the activated carbon which is expensive and has high regeneration cost [5]. Therefore, many researchers have studied dye adsorption by different

*Corresponding authors.

low-cost adsorbents such as agricultural byproduct, industrial waste, and natural and modified clays [6,7].

Agricultural by-products such as peanut husk, apple pomace, wheat straw and wheat shell, cereal chaff, fruit peel, bark and leaves, banana pith, banana peel, plum kernels, sawdust, coir pith, sugarcane bagasse, tea leaves, bamboo dust, etc. have been widely studied for removal of dyes from wastewater [8–11]. However, the application of untreated plant wastes as adsorbents can also bring several problems such as lower adsorption capacity, higher chemical oxygen demand (COD), and biological chemical demand (BOD) as well as total organic carbon (TOC) due to release of soluble organic compounds contained in the plant materials [12]. Therefore, plant wastes need to be modified or treated before being applied for the decontamination of dyes. Pretreatment methods using different kinds of modifying agents such as base solutions (sodium hydroxide) mineral and organic acid solutions (hydrochloric acid, phosphoric acid, tartaric acid, citric acid, and thioglycollic acid), organic compounds (ethylenediamine and formaldehyde), etc. for the purpose of removing soluble organic compounds, eliminating color of the aqueous solutions, and increasing efficiency of dye adsorption have been performed by many researchers [13–16]. Modification of agricultural by-products can be carried out to achieve adequate structural durability, enhance their natural ion exchange capability and add value to the by-product [17]. Low et al. [18] used esterifying wood to adsorb copper and lead. The maximum adsorption capacities increased 10 folds compared to untreated wood. Vaughan et al. [19] modified corncobs with citric acid and reported adsorption efficiency with five different metal ions (cadmium, copper, lead, nickel, and zinc). The result showed that modified corncobs had the same adsorption efficiency as Duolite GT-73 for cadmium, copper, nickel, and zinc ions and had greater adsorption than CMC for nickel and zinc ions. Gong and coworkers [13] employed esterifying rice straw for enhancing malachite green removal. They also reported the adsorption behavior of methylene blue and crystal violet on citric acid esterifying wheat straw. The maximum adsorption capacity for MB and CV was 312.50 and 227.27 mg/g, respectively [13].

Peanut is an oil plant which is extensively cultured in China. Peanut husk is an abundant and inexpensive agricultural by-product. Most of this agricultural by-product is arbitrarily discarded or set on fire. These disposals must result in environmental pollution. It contains abundant lignin, cellulose, and some functional groups such as carboxyl, hydroxyl, phenolic, and amide groups, etc. in its structure, so it can be utilized for dyes and heavy metals removal as it can also bring unlimited number of economic and environmental benefits to the industrial wastewater treatment [20,21]. However, the studies on the use of citric acid modified peanut husk as an adsorbent in removal dyes from solutions are limited, and in the previous studies, only single component systems were investigated, and a few investigations on binary systems have been reported to consider competitive adsorption using modified plant materials. Understanding of multicomponent interaction with adsorbent would be very helpful for its use in wastewater treatment.

Thermochemical esterifying citric acid on peanut husk can enhance peanut husk ability of cationic dye adsorption. When heated, citric acid will dehydrate to yield a reactive anhydride which can react with the hydroxyl groups on the cellulose to form an ester linkage. The introduced free carboxyl groups of citric acid onto plant material surfaces increase the net negative charge on the peanut husk fiber, thereby increasing its binding potential for cationic contaminants [13,19].

To observe the potential feasibility of removing color, peanut husk was modified with citric acid and used for adsorption of cationic dyes from aqueous solution. The dyes selected as adsorbate were neutral red (C.I.50040, FW = 288.8, λ_{max} = 530 nm) and methylene blue (C.I.52015, FW = 373.9, λ_{max} = 660 nm). In this paper, an investigation of coadsorption of neutral red (NB) and methylene blue (MB) is presented. We compare their adsorption in single and binary systems to investigate simultaneous adsorption processes and determine the adsorption kinetics and equilibrium in single systems. Further, the kinetics and the mechanistic steps involved in the sorption process were evaluated at different temperatures. The adsorption capacity of the adsorbents used in the present work was also compared with other adsorbents used by different researchers.

2. Materials and methods

2.1. Preparation of MPH

Fresh biomass of peanut husk was collected from its natural habitats in the farmland, Luoyang City, China. It was washed a few times with distilled water, dried for 8 h at 60°C in the oven. The dry peanut husk was crushed into powder and sieved to 20–40 mesh fractions for chemical modification.

MPH was prepared according to the modified method [19]. Ground peanut husk was mixed with 0.6 mol/L citric acid at the ratio of 1:12 (peanut husk/acid, w/v) and stirred for 30 min at 20°C. The acid

peanut husk slurries were placed in a stainless steel tray and dried at 50°C in a forced air oven for 24 h. Then the thermochemical esterification between acid and peanut husk was enhanced by raising the oven temperature to 120°C for 90 min. After cooling, the esterified peanut husk was washed with distilled water until the liquid did not turn turbidity when 0.1 mol/L $Pb(NO_3)_2$ was dropped in. After filtration, MPH was suspended in 0.1 mol/L NaOH solution at suitable ratio and stirred for 60 min, followed by washing thoroughly with distilled water to remove residual alkali, next dried at 50°C for 24 h and preserved in a desiccator for use.

The chemical modification of peanut husk may be expressed schematically as [19]:

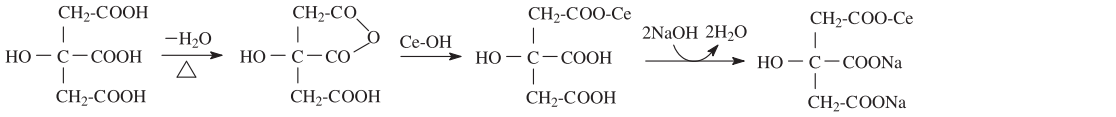

where Ce-OH corresponds to natural peanut husk.

The determination of pH_{zpc} of MPH was performed according to the solid addition method [22]: 20 mL of 0.01 mol/L KNO_3 solution was placed in conical flasks. The initial pH of the solutions was adjusted to a value between 2 and 11 by adding 1 mol/L HCl or NaOH solution. Then 0.1 g of MPH was added to each flask, stirred, and the final pH of the solutions was measured after 24 h. The value of pH_{zpc} can be determined from the curve that cuts the pH_i line of the plot ΔpH vs. pH_i. The plot of change in solution pH (ΔpH) vs. initial pH (pH_i) showed that with increasing initial solution pH, the pH change become more negative and the zero value of ΔpH was reached at pH_i value of 4.21, which is considered as the pH_{zpc} of MPH (shown in Fig. 2).

2.2. Preparation of cationic dyes solution

All the chemicals used in this work were analytical grade reagents with deionized water used for solution preparation. The dyes of NR and MB were obtained from the Luoyang Chemical Corporation in China. The NR and MB stock solutions were prepared by dissolving accurately weighted dye in distilled water to the concentration of 1,000 mg/L, respectively. The experimental solutions were obtained by diluting the dye stock solution in accurate proportions to different initial concentrations. As experiment result proved that the optional value of solution pH for NR and MB is 5 and 7, respectively, the initial pH of the working solution was adjusted by addition of 1 mol/L HCl or NaOH solution.

2.3. Experimental methods and measurements

The adsorption of two cationic dyes on MPH was investigated in batch mode adsorption equilibrium experiments. All batch experiments were carried out in 50 mL flasks containing a fixed amount of adsorbent with 10 mL dye solution at a known initial concentration. The flasks were agitated at a constant speed of 100 rpm for 480 min in an orbital shaker. For isothermal studies, a series of 50 mL flasks were used and each flask was filled with MPH at mass loadings 3 g/L for NR or MB solutions with different initial concentrations varying from 10 to 500 mg/L at 283, 298, and 313 K, respectively. Biosorption kinetic study was conducted with a known initial dyes concentration at temperatures of 283, 293 and 303 K, respectively. Samples were collected at various shaking time intervals until the concentration of dyes in the dilute phase became constant. The effect of pH on adsorption of MB onto MPH was investigated by varying the solution initial pH from 2.0 to 10.00. As NR is precipitated when pH is above 7 in an experiment, the effect of pH on NR removal was analyzed over the pH range from 1 to 7. The pH was adjusted using 1 mol/L NaOH or HCl solutions. The effects of the ionic strength of NaCl or $CaCl_2$ solution (0.01–0.1 mol/L) on dyes uptake were then examined. For binary systems, MPH at loadings of 3 g/L was mixed with NR and MB mixture solutions at various initial concentrations. The contact time was 480 min.

Concentrations in aqueous solution were determined spectrophotometrically in the visible range of the spectrum. After adsorption, the adsorbent was separated by filtering. For single component systems, concentrations were measured based on the solution absorbance (A) at wavelengths corresponding to the maximum absorbance by NR and MB. The concentration of dyes in solution was performed on a UV/Vis-3000 spectrophotometer (Shimadzu Brand UV-3000, with a 1-cm path length) at a wavelength of maximum absorbance of 530 and 660 nm for NR and MB, respectively. Each experiment was repeated three times and the results given were the average value.

For the binary system, the dye concentrations were measured using the following formula:

$$A_{530} = k_{NR(530)} b C_{NR} + k_{MB(530)} b C_{MB} \quad (1)$$

$$A_{660} = k_{NR(660)} b C_{NR} + k_{MB(660)} b C_{MB} \quad (2)$$

where A is the absorbance for mixture solution, k is the absorption coefficient (L/mg cm), and b is light path length through solution.

The amount of dye adsorbed onto unit weight of adsorbent (q) was calculated using the following equation:

$$q = \frac{V(C_0 - C)}{1000m} \quad (3)$$

where V is the solution volume in L, C_0 is the initial dye concentration in mg/L, C is the dye concentration at any time in mg/L, and m is the dry weight of MPH in g.

2.4. Regeneration studies

In order to determine the reusability of MPH, consecutive adsorption–desorption cycles were repeated three times. The solution of 0.1 mol/L HCl was used as the desorbing agent. The MPH loaded with NR or MB was placed in the desorbing medium and was constantly stirred on a rotatory shaker at 100 rpm for 120 min at 283 K. After each cycle of adsorption and desorption, the adsorbent was washed with distilled water and reconditioned for adsorption in the succeeding cycle.

3. Results and discussion

3.1. FTIR of NPH and MPH

Like all vegetable biomass, peanut husks are composed of cellulose (34–45%), lignin (27–33%), fiber (60–70%), protein (6–7%), moisture (8–10%), fat (1%), and ash (2–4%) [23]. From elemental analysis, the contents (%, of total matter) were obtained for carbon (45.49), hydrogen (5.93), oxygen (34.41), and nitrogen (1.26) [24]. Peanut husks, mainly consisted of polysaccharides, proteins, and lipids, offer many polar functional groups such as carboxyl, carbonyl, hydroxyl, and amino groups which can be involved in dye binding. The pattern of adsorption of ions onto plant materials was attributable to the active groups and bonds present on them.

The FTIR technique is an important tool to identify some characteristic functional groups, which are capable of adsorbing dye ions [25]. The FTIR of NPH and MPH was shown in Fig. 1. As shown in Fig. 1, the spectra displayed a number of absorption peaks, indicating the complex nature of the material. The broad band around 3,426 cm^{-1} was attributed to the surface

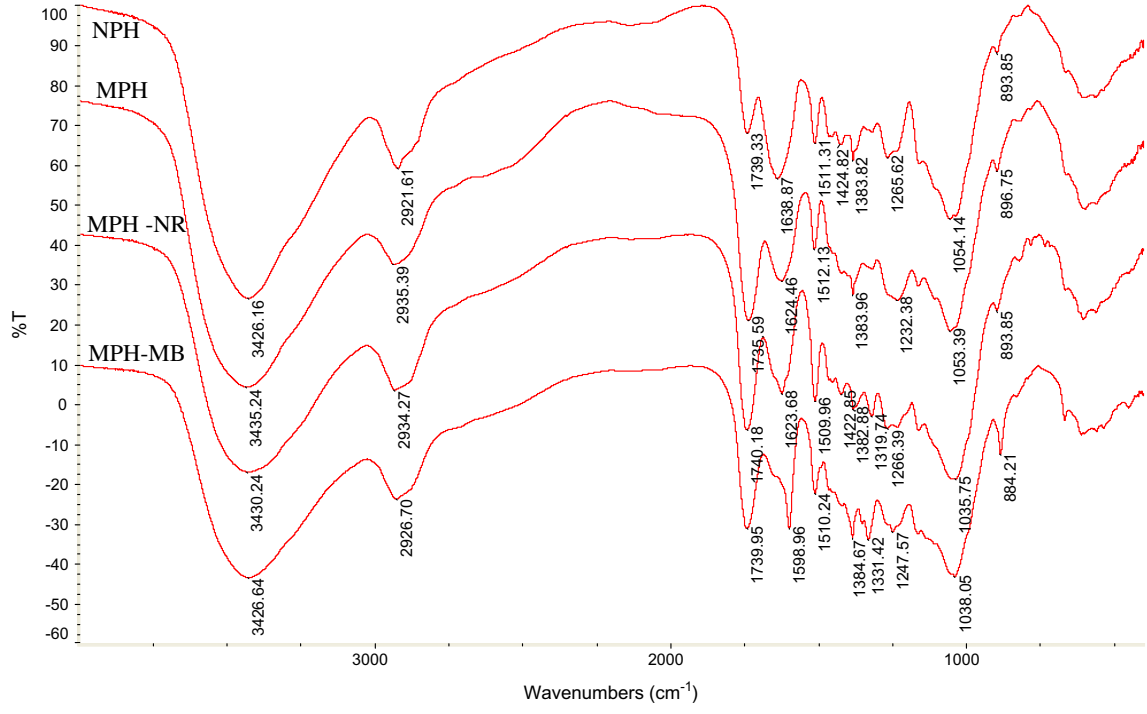

Fig. 1. Fourier transform infrared spectra of natural peanut husk (NPH), modified peanut husk (MPH), and modified peanut husk (MPH) adsorbed NR and MB.

hydroxyl groups, adsorbed water, and amine groups. The O–H stretching vibrations occurred within a broad range of frequencies indicating the presence of "free" hydroxyl groups and bonded O–H bands of carboxylic acids. The peaks observed at 2,927 and 1,383 cm^{-1} were assigned to the stretch vibration and bending vibration of C–H bond in methyl group, respectively. These groups were present on the lignin structure [25]. The peaks located at 1,739 and 1,638 cm^{-1} were characteristics of the carbonyl group stretching from carboxylic acids and ketones. They could be conjugated or nonconjugated to aromatic rings (1,739 and 1,638 cm^{-1}, respectively). The peaks associated with the stretching in aromatic rings (from lignin) were verified at 1,511 cm^{-1}. The peak near 1,423 cm^{-1} was attributed to the stretch vibration of C–O from the carboxyl group. The peak at 1265 cm^{-1} is indicative of the OH in-plane bending cellulose. The wave number observed at 1,054 cm^{-1} was due to the C–O group in carboxylic and alcoholic groups [25].

From Fig. 1, it is shown that modification brought increase of stretch vibration adsorption band of carboxyl group (at 1,735 cm^{-1}). The shift of some peaks changed after modification. The results showed that MPH had more carboxyl groups than NPH. The intensity is a function of the change in electric dipole moment and also the total number of such bonds in the sample. The band of C–O group is more intense than that of C=O group, possibly because of more C–O groups present in the modified peanut husk [25]. These groups may function as proton donors, hence deprotonated hydroxyl and carboxyl groups may be involved in coordination with positive dye ions. Dissolved NR and MB ions are positively charged and will undergo attraction on approaching the anionic MPH structure. On this basis, it is expected that an NR and MB ions will have a strong sorption affinity by MPH.

It was observed from Fig. 1 that after adsorbing NR and MB on MPH, there were slight changes in the absorption peak frequencies, which suggested that there was a binding process taking place on the surface of the adsorbent. As seen in Fig. 1, after adsorbing MB on MPH, vibration strength of three peaks, 1,599, 1,331, and 884 cm^{-1} (which indicated the bonded C–O groups, aromatic nitro compound, and C–C group) significantly increased. For NR-loaded MPH, strength of peak at 1,509 cm^{-1} also increased. This change was contributed to dye molecular adsorbed onto surface of adsorbent. The above results obtained give an idea about the presence of functional groups on the MPH surfaces and also the mechanism of adsorption, which is dependent on functional groups especially carboxyl groups.

3.2. Effect of initial pH

The pH_{zpc} of an adsorbent is a very important characteristic that determines the pH at which the adsorbent surface has net electrical neutrality. Fig. 2 illustrates the point of zero charge (pzc) of MPH. The pH_{pzc} of MPH was found to be 4.21.

Initial pH value of solution is one of the most important factors influencing the dye adsorption. This is because hydrogen ion competing with the positively charged dye ions on the active sites of the adsorbent. Fig. 3 shows the effect of initial solution pH on the percent color removal of NR and MB adsorbed at equilibrium conditions. As shown in Fig. 3, the uptake of two dye ions depends on pH, it increases with the increase in pH reaching the maximum adsorption at 5.0 and 7.8 for NR and MB, respectively. On higher

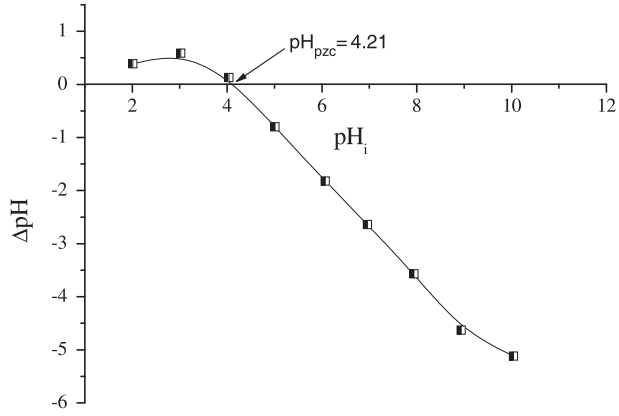

Fig. 2. The variation of point of zero charge with equilibrium pH of MPH suspensions.

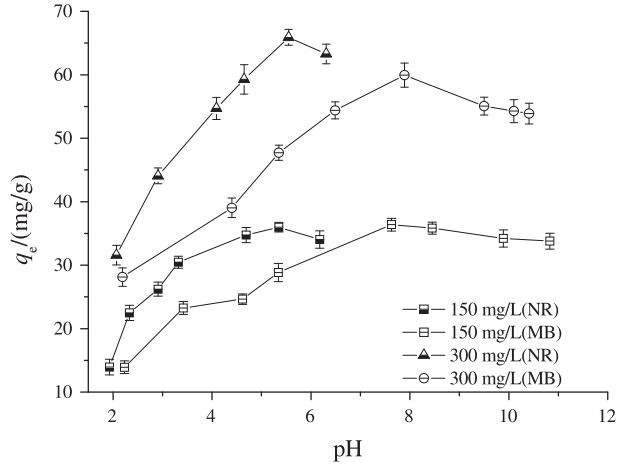

Fig. 3. Effect of the initial solution pH on the removal of NR and MB by MPH ($C_{o(NR)}$ = 150 mg/L; 300 mg/L, $C_{o(MB)}$ = 150 mg/L; 300 mg/L, MPH dosage = 3 g/L, contact time = 480 min, 283 K).

pH values, a slight decrease of adsorption for NR and MB ions was observed. The values of q_e for MPH were the smallest at the initial pH 2.0. Because of the varying amounts and nature of surface oxygen, adsorbents of MPH should be regarded as a special case of amphoteric solids. Both negative and positively charged surface sites exist in aqueous solution, depending on the solution pH. When solution $pH < pH_{zpc}$, the surface of MPH is positively charged and attractive to anions. The practical functional group of MPH is carboxyl group. The presence of excess H^+ ions could restrain the ionization of the carboxyl group, so the nonionic form of carboxyl group, –COOH, was presented. The adsorption capacity of dye ions was small because of the absence of electrostatic interaction. When solution $pH > pH_{zpc}$, the surface of MPH is negatively charges and can attract cations from the solution. The carboxyl group is turned into $–COO^-$, a significantly high electrostatic attraction exists between the negatively charged surface of MPH and cationic dye molecules, leading to maximum dye adsorption. Similar results were reported for the adsorption of cationic dye from aqueous solution on biosorbent [25].

3.3. Effect of NaCl and $CaCl_2$ concentration on adsorption

Different amount of various salts present in the dye-laden wastewaters, these salts can result in a high ionic strength which may affect the performance of the adsorption process. In this study, a series of NaCl and $CaCl_2$ solutions, ranging in concentration were employed as background solutions to study the effect of salt concentration, as well as the effect of competitive ions on the adsorption of NR and MB.

Fig. 4 shows the influence of NaCl and $CaCl_2$ on the adsorption of NR and MB onto MPH. In the absence of salt, the adsorption capacity of NR was 37.3 and 61.8 mg/g at the initial concentration of 150 and 300 mg/L, respectively. And the adsorption capacity of MB was 31.2 and 50.1 mg/g at the initial concentration of 150 and 300 mg/L, respectively. However, increasing the salt concentration led to a decrease of NR and MB adsorption on MPH. The uptake of NR and MB decreased from 37.3 and 31.2 mg/g to 29.9 and 21.6 mg/g for an increase in NaCl concentration from 0.01 to 0.10 mol/L (the initial concentration of NR and MB was 150 mg/L), respectively. While the uptake of NR and MB decreased from rom 37.3 and 31.2 mg/g to 19.4 and 8.0 mg/g in the presence of $CaCl_2$, respectively. This suggests that $CaCl_2$ induced a greater suppression effect over NR and MB ions than NaCl under the concentration range

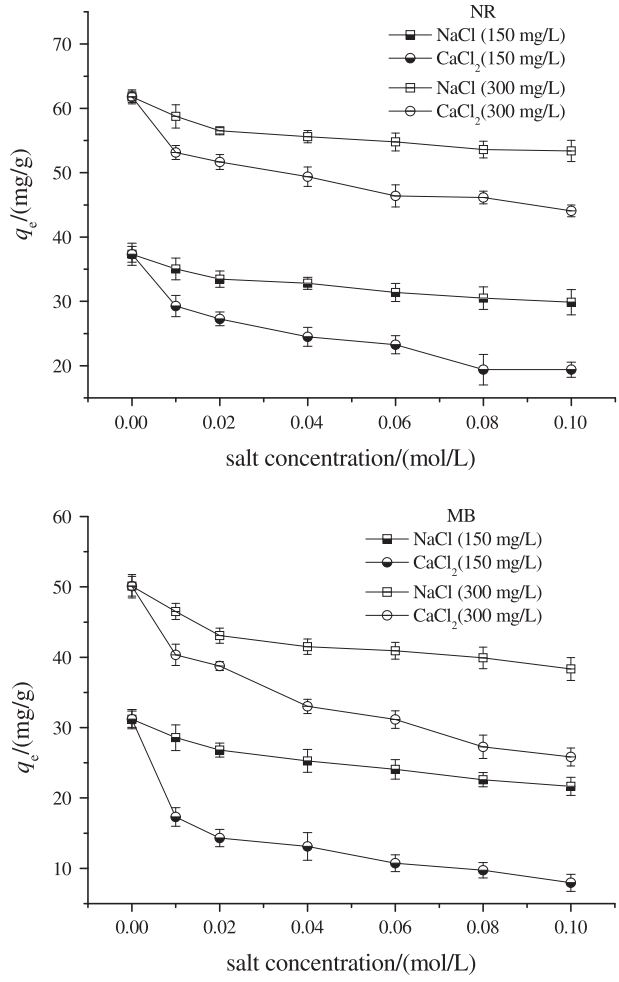

Fig. 4. The effect of NaCl and $CaCl_2$ concentration on adsorption ($C_{o(NR)}$ = 150 mg/L; 300 mg/L, $C_{o(MB)}$ = 150 mg/L; 300 mg/L, MPH dosage = 3 g/L, contact time = 480 min, 283 K).

studied. In general, the reduction in cationic dyes uptake in NaCl or $CaCl_2$ electrolyte solutions can be explained in terms of two aspects: first, the competitive effect of Na^+ and Ca^{2+} for binding sites and second, the expansion of the electrical diffused double layer. Such expansion could inhibit the adsorbent and metal ions from approaching each other, and a decrease in electrostatic attraction would be expected [25]. As Ca^{2+} has more contribution to ionic strength and more positive charge than Na^+, the effect of Ca^{2+} on adsorption is more serious than Na^+ in the same mole concentration.

3.4. Adsorption kinetic study

Fig. 5 illustrates the effect of contact time on adsorption of NR and MB on MPH at different tem-

perature. From Fig. 5, it was found that the adsorptive quantity of both NR and MB on MPH increased with the contact time increasing. A two-stage kinetic behavior was evident: an initial rapid stage where adsorption was fast and contributed significant to equilibrium uptake and a slower second stage whose contribution to the total NR and MB adsorption was relatively small.

It was also seen from Fig. 5 that higher temperature was advantage of the increase in adsorption quantity. This indicated that the adsorption of NR and MB ions onto MPH was endothermic in nature. The increase in adsorption with temperature may be attributed to either increase in the number of active surface sites available for sorption on the adsorbent or due to the decrease in the boundary layer thickness surrounding the sorbent, so that the mass transfer resistance of adsorbate in the boundary layer decreased [26].

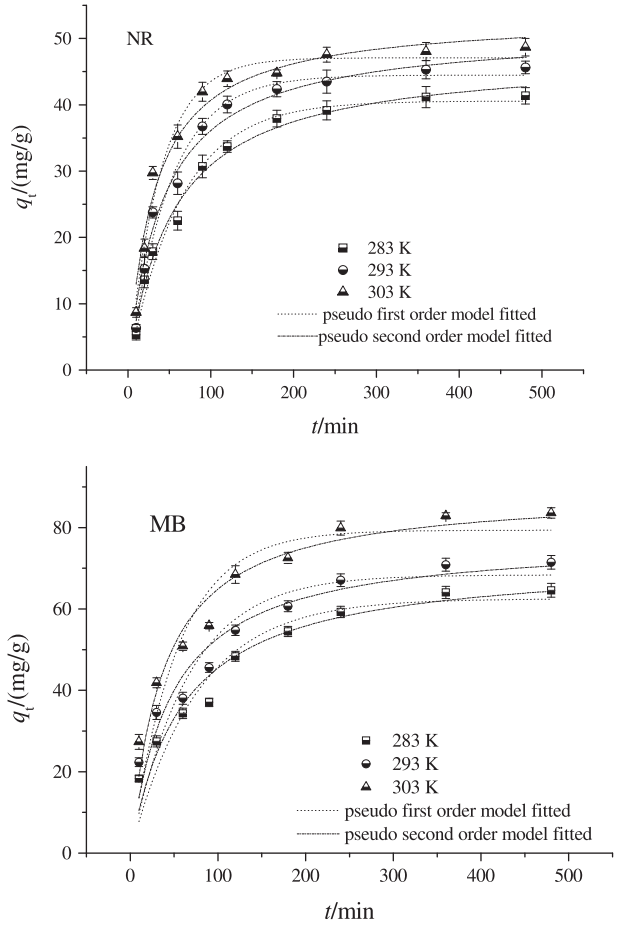

Fig. 5. The effect of contacting time on adsorption of NR (C_o = 150 mg/L) and MB (C_o = 300 mg/L) by MPH (MPH dosage = 3 g/L).

In order to analyze the adsorption kinetics for the adsorption of NR and MB, the pseudo-first-order kinetic model, pseudo-second-order kinetic model, and intraparticle diffusion model were applied.

The pseudo-first-order kinetic model is expressed as [27]:

$$q_t = q_e(1 - e^{-k_1 t}) \tag{4}$$

The pseudo-second-order kinetic model is given by the following equation as [27]:

$$q_t = \frac{k_2 q_e^2 t}{1 + k_2 q_e t} \tag{5}$$

where q_e and q_t are the amount of dyes adsorbed per unit weight of the adsorbent at equilibrium and at any time t, respectively (mg/g), k_1 is the rate constant of pseudo-first-order adsorption (1/min); and k_2 is the rate constant of pseudo-second-order adsorption (g/mg min).

Table 1 presents the results of fitting experimental data with pseudo-first-order and pseudo-second-order equations using nonlinear analysis. The fitted curves are also shown in Fig. 5.

From Table 1, it was found that the values of q_e, k_1, and k_2 increased with when temperature increased for both NR and MB adsorption. The values of R^2 (bigger than 0.97) and χ^2 (less than 2.50) for NR are slightly different for pseudo-first-order equation and pseudo-second-order equation, respectively. The calculated values of q_e obtained from pseudo-first-order model and pseudo-second-order model agreed more perfectly with the experimental $q_{e(exp)}$ values of NR adsorption at three different temperatures, respectively. So it is concluded that two models can predict the kinetic process of NR on MPH in experimental condition.

But for MB adsorption, pseudo-second-order kinetic model is better to fit the whole adsorption process according to the values of R^2 and χ^2. Fig. 5 typically illustrates the comparison between the calculated and measured results for the adsorption of NR and MB onto MPH.

From the plots of pseudo-second-order kinetic model, $k_2 q_e^2$ known as the initial adsorption rate was also obtained, for NR (0.881, 1.212, and 1.711 mg/g min) and for MB (1.796, 2.391, and 3.842 mg/g min) at different temperatures, respectively. The value of $k_2 q_e^2$ and q_e indicates higher temperature that favors the adsorption process by increasing adsorption rate and capacity.

Table 1
Kinetic parameters of NR and MB adsorption onto MPH

T/K	283 K	293 K	303 K
NR			
Pseudo-first-order model			
k_1/(1/min)	0.016 ± 0.001	0.020 ± 0.002	0.026 ± 0.002
$q_{e(cal)}$/(mg/g)	40.57 ± 0.920	44.47 ± 0.984	47.08 ± 0.991
$q_{e(exp)}$/(mg/g)	41.36	45.63	48.68
R^2	0.9857	0.9830	0.9793
χ^2 [a]	1.313	1.427	1.426
Pseudo-second-order model			
k_2/(g/mg min)×10^4	3.90 ± 0.50	4.60 ± 0.70	6.00 ± 0.10
$q_{e(cal)}$/(mg/g)	47.54 ± 1.362	51.32 ± 1.673	53.40 ± 1.744
R^2	0.9879	0.9798	0.9715
χ^2	1.091	2.000	2.456
Intraparticle diffusion model			
C_1/(mg/g)	−1.327 ± 0.851	−3.615 ± 0.691	−3.014 ± 1.014
K_{t1}/(mg/g min)	2.985 ± 0.096	3.861 ± 0.100	4.662 ± 0.156
C_2/(mg/g)	32.644 ± 3.477	37.361 ± 3.083	38.319 ± 1.937
K_{t2}/(mg/g min)	0.412 ± 0.195	0.387 ± 0.166	0.500 ± 0.131
MB			
Pseudo-first-order model			
k_1/(1/min)	0.020 ± 0.0038	0.025 ± 0.0048	0.029 ± 0.0049
$q_{e(cal)}$/(mg/g)	59.83 ± 2.96	65.82 ± 3.29	77.46 ± 3.21
$q_{e(exp)}$/(mg/g)	64.58	71.48	83.59
R^2	0.8971	0.8713	0.8954
χ^2	10.389	10.108	7.811
Pseudo-second-order model			
k_2/(g/mg min)×10^4	3.90 ± 0.70	4.40 ± 0.90	5.20 ± 0.60
$q_{e(cal)}$/(mg/g)	67.86 ± 2.59	73.72 ± 2.80	85.96 ± 2.22
R^2	0.9655	0.9561	0.9752
χ^2	2.803	3.159	1.639
Intraparticle diffusion model			
C_1/(mg/g)	9.351 ± 0.804	14.821 ± 1.125	25.789 ± 1.184
K_{t1}/(mg/g min)	3.413 ± 0.096	3.526 ± 0.120	3.655 ± 0.135
C_2/(mg/g)	46.093 ± 6.289	56.472 ± 6.669	72.388 ± 6.315
K_{t2}/(mg/g min)	0.882 ± 0.338	0.710 ± 0.354	0.535 ± 0.327

[a] $\chi^2 = \sum \frac{(q_{e,exp} - q_{e,cal})^2}{q_{e,cal}}$, $q_{e,exp}$ and $q_{e,cal}$ are the experimental value and calculated value according the model, respectively.

3.5. Mechanism of adsorption

For practical applications of adsorption such as process design and control, it is important to understand the dynamic behavior of the system. However the determination of the sorption mechanism is also important for design purposes. In a solid-liquid adsorption process, the adsorbate transport from the solution phase to the surface of the adsorbent particles is characterized by either boundary-layer diffusion (external mass transfer) or intraparticle diffusion (mass transfer through the pores), or by both. It is generally accepted that the adsorption dynamics consists of three consecutive steps, e.g. film or external diffusion, pore diffusion, adsorption on the pore surface, or a combination of more than one step. The last step, adsorption, is usually very rapid in comparison to the first two steps. Therefore, the overall rate of adsorption is controlled by either film or intraparticle diffusion, or a combination of both.

The possibility of intraparticle diffusion was explored by using the intra-particle diffusion model [28]:

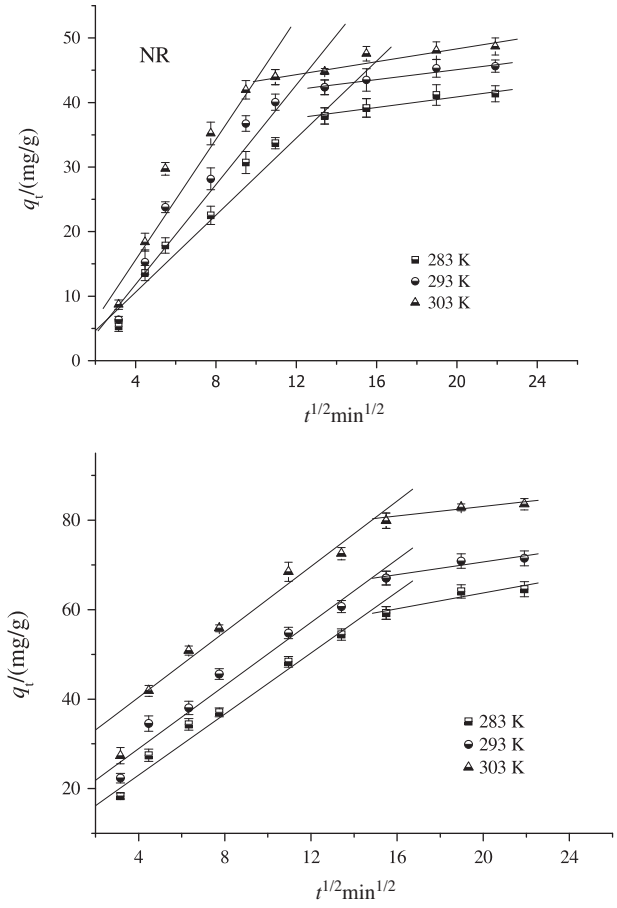

Fig. 6. Intraparticle diffusion plots for NR and MB adsorption of onto MPH.

$$q_t = K_t t^{1/2} + C \quad (6)$$

K_t is the intraparticle diffusion rate constant (g/mg min$^{1/2}$), C is a constant that gives idea about the thickness of the boundary layer, i.e. larger the value of C the greater is the boundary layer effect.

If the plot of q_t vs. $t^{1/2}$ gives a straight line, then the sorption process is controlled by intraparticle diffusion only. However, if the data exhibit multilinear plots, then two or more steps influence the sorption process. It is assumed that the external resistance to mass transfer surrounding the particles is significant only in the early stages of adsorption. This is represented by first sharper portion. The second or third linear portion is the gradual adsorption stage with intraparticle diffusion dominating.

Fig. 6 presents the plots of q_t vs. $t^{1/2}$ for NR and MB adsorption. In Fig. 6, the data points were related by two straight lines for NR and MB, respectively. The first straight portion depicted macropore diffusion and the second represented micropore diffusion [29]. But the micropores (pores with a width less than 2 nm) are rather not accessible to large molecules of dyes. However, when MPH was modified with citric acid, the pore size of micropore on MPH may be enlarged and the mesopores (2–50 nm) would be produced. The mesopores could be accessible to large molecules of dyes. This effect may be attributed to the enlargement of pore size. The values of K_t and C are also listed in Table 1. From Table 1, the constants of C were not zero the lines did not pass through the origin. This showed that pore diffusion was not the rate limiting step. So the adsorption process may be of a complex nature consisting of both surface adsorption and intraparticle diffusion [29]. Furthermore, all these suggest that the adsorption of NR and MB over MPH may be controlled by external mass transfer followed by intraparticle diffusion mass transfer.

Obviously, K_{t1} is larger than K_{t2} from Table 1 while C_1 is smaller than C_2. As mentioned above, initially, the dyes were adsorbed by the external surface of the adsorbent, so the adsorption rate was very fast. When the adsorption of the external surface reached saturation, the dye molecule entered into the pores within the particle and eventually was adsorbed on the active sites of the adsorbent internal surface. When the dye molecule transported in the pore of the particle, the diffusion resistance increased and consequently reduced the diffusion rate. With the decrease of the dye concentration in the solution, the diffusion rate became much smaller and the diffusion processes reached the final equilibrium stage.

In order to corroborate the actual rate controlling steps in NR and MB adsorption on MPH, the experimental data were further analyzed by the expression of Boyd et al. [30]:

$$F = 1 - \left(\frac{6}{\pi^2}\right)\exp(-Bt) \quad (7)$$

where F is the fractional attainment of equilibrium, at different times, t, and Bt is a function of F.

$$F = \frac{q_t}{q_e} \quad (8)$$

where q_t and q_e are the dyes uptake (mg/g) at time t and at equilibrium, respectively. Eq. (7) can be rearranged to

$$Bt = -0.4997 - \ln\left(1 - \frac{q_t}{q_e}\right) \quad (9)$$

Values of B were calculated from the slope of Bt vs. time plots. The calculated values of B were used to determine the effective diffusion coefficient, D_i (cm^2/s) of NR and MB from the equation:

$$B = \frac{\pi^2 D_i}{r^2} \tag{10}$$

where r is the radius of the adsorbent particle assuming spherical shape (20–40 mesh, 30 mesh was chosen). According to Singh et al. [31], a D_i value in the order of 10^{-10}–10^{-11} cm^2/s is indicative of intraparticle diffusion as rate-limiting step. In this study, the values of D_i for NR were 8.88×10^{-8}, 8.16×10^{-8} and 7.47×10^{-8} cm^2/s, and for MB were 7.46×10^{-8}, 7.36×10^{-8} and 7.47×10^{-8} cm^2/s at 283, 293, and 303 K, respectively. The values of D_i of NR and MB obtained are in the order of 10^{-8} cm^2/s, respectively, which is larger than 3 orders of magnitude. This indicates that the intraparticle diffusion is not the rate-controlling step.

3.6. Effect of equilibrium concentration of NR and MB adsorption on temperature-dependent adsorption

The effect of initial dye concentration on NR and MB adsorption by MPH was investigated in the range of 50–500 mg/L. Fig. 7 shows the equilibrium quantity at different initial dyes concentration.

From Fig. 7, the values of q_e increased with increase in C_e. The initial concentration provided the necessary driving force to overcome the resistances to the mass transfer of dyes between the aqueous and solid phases. The increase in C_e also enhanced the interaction between dyes and adsorbents. Therefore, an increase in C_e of dyes enhanced the adsorption uptake of NR or MB.

The bigger adsorptive capacity of dyes was also observed in the higher temperature range. This was due to the increasing tendency of adsorbate ions to adsorb from the solution to the interface with increasing temperature. The increase in the equilibrium adsorption with increased temperature indicated that the adsorption of dye ions onto MPH is endothermic in nature.

Analysis of adsorption isotherms is important for developing a model that can be used for adsorption process design, and the isotherms obtained under different temperatures can provide basic data for thermodynamics study to deduce adsorption mechanism. In the present work, the results obtained from the equilibrium adsorption experiments were analyzed according to the most frequently employed models Freundlich and Langmuir isotherms at the temperatures of 283, 298, and 313 K, respectively.

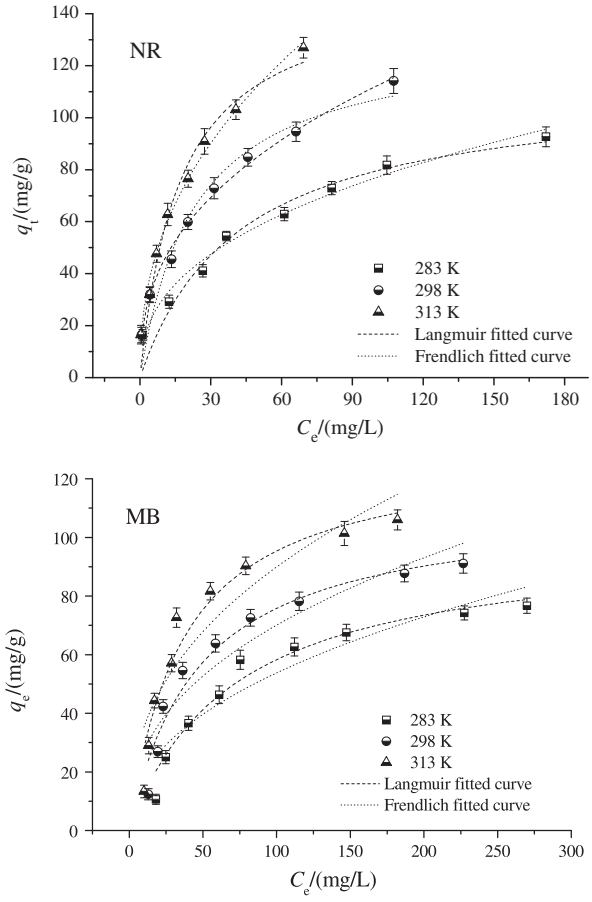

Fig. 7. Equilibrium adsorption quantities of NR and MB adsorption at different equilibrium dyes concentration and predicted isotherm curves (MPH doseage = 3 g/L).

The Langmuir adsorption isotherm has been successfully applied to many pollutants adsorption processes and has been the most widely used sorption isotherm for the sorption of a solute from a liquid solution [32]. The commonly form of the Langmuir isotherm is:

$$q_e = \frac{q_m K_L C_e}{1 + K_L C_e} \tag{11}$$

where q_m is the q_e for a complete monolayer (mg/g), a constant related to adsorption capacity; and K_L is a constant related to the affinity of the binding sites and energy of adsorption (L/mg).

Freundlich isotherm is an empirical equation describing adsorption onto a heterogeneous surface. The Freundlich isotherm is commonly presented as [33]:

$$q_e = K_F C_e^{1/n} \tag{12}$$

Table 2
Langmuir and Freundlich isotherm constants for NR and MB adsorption onto MPH at different temperatures using nonlinear regressive method

Dye	Model	283 K	298 K	313 K
NR	Langmuir			
	K_L	0.024 ± 0.006	0.043 ± 0.011	0.058 ± 0.012
	q_m (mg/g)	112.72 ± 10.68	131.86 ± 12.51	151.24 ± 11.49
	R^2	0.9528	0.9523	0.9729
	χ^2	65.72	48.64	42.90
	Freundlich			
	K_F	12.17 ± 1.56	17.89 ± 1.08	20.87 ± 1.50
	$1/n$	0.400 ± 0.028	0.398 ± 0.015	0.430 ± 0.020
	R^2	0.9829	0.9950	0.9921
	χ^2	2.540	0.688	1.668
MB	Langmuir			
	K_L	0.014 ± 0.003	0.021 ± 0.004	0.028 ± 0.006
	q_m (mg/g)	99.41 ± 7.12	111.38 ± 7.59	129.83 ± 9.80
	R^2	0.9636	0.9589	0.9507
	χ^2	5.674	8.267	11.391
	Freundlich			
	K_F	7.13 ± 2.43	12.59 ± 3.22	13.86 ± 4.26
	$1/n$	0.439 ± 0.068	0.410 ± 0.064	0.406 ± 0.068
	R^2	0.8897	0.8869	0.8650
	χ^2	13.33	31.86	24.47

where K_F and $1/n$ are the Freundlich constants related to the adsorption capacity and adsorption intensity of the adsorbent, respectively.

All relative parameters of isotherm equation and determined coefficients (R^2), values of χ^2 are listed in Table 2, respectively. Fig. 7 also shows the experimental equilibrium data and fitted equilibrium curves by two isotherms at different temperature, respectively.

From Table 2, the values of q_m, K_L, and K_F increased with temperature rise for NR and MB adsorption, respectively. The maximal equilibrium quantity of NR and MB from Langmuir model on MPH was 112.72 ± 10.68 mg/g (0.390 ± 0.037 mmol/g) and 99.41 ± 7.12 mg/g (0.266 ± 0.019 mmol/g) at 283 K, respectively. The values of q_m obtained from the Langmuir isotherm equation for NR adsorption on MPH was greater than that of MB at all the temperature, which is indicated that the functional groups on the surface of MPH had a relatively stronger affinity for NR than MB and potential of the adsorption for NR and MB on MPH was in the following order: NR > MB.

The values of $1/n$ for both dyes were below 1 at all the experimental temperatures, which indicate high adsorption intensity [33]. The Freundlich constant, K_F, which are related to the adsorption capacity, also shows that the adsorption capacity increased with increase in temperature, indicating that the adsorption processes are endothermic in nature.

From values of R^2 and χ^2, it can be seen that the Langmuir isotherm exhibited a better fit to the MB adsorption data by MPH while the Freundlich isotherm seem to agree better with the NR adsorption. The comparison of experimental points and fitted curves in Fig. 7 reinforced this result. It can be seen that the Langmuir isotherm correlated better than Freundlich isotherm with the experimental data from adsorption equilibrium of MB by MPH, suggesting a monolayer adsorption. In comparison, the Freundlich correlation coefficients of NR adsorption were larger than those of Langmuir, which indicated the adsorption of NR is a heterogeneous adsorption.

Table 3 compares the sorption capacities of the MPH for NR and MB with that of several adsorbents reported in the literatures. It can be seen that the MPH exhibits higher uptake properties of both NR and MB than that of many other sorbents. The results reveal that MPH has a good potential for NR and MB ion removal from waste water.

3.7. Estimation of thermodynamic parameters

3.7.1. Calculation of the change free energy change (ΔG)

Thermodynamics parameters are important in adsorption studies for better understanding of the tem-

Table 3
Comparison of the adsorption capacity for NR and MB by various adsorbents reported in literature

Adsorbent	Adsorption capacity/(mg/g)	References
NR		
MPH	112.72	This study
Peanut husk	35.7	[7]
Cottonseed hull	166.7	[34]
Kohlrabi peel	112.36	[34]
Peanut hull	87.72	[19]
Rice husk	32.37	[36]
Modified hectorite	393.7	[37]
Activated carbon from cattail	192.30	[38]
MB		
MPH	99.21	This study
Rice husk	40.6	[29]
Cereal chaff	20.3	[9]
Peanut hull	68.03	[19]
Coconut husk	99	[39]
Wheat bran	16.63	[40]
Olive pomace	42.3	[41]
Phoenix tree leaves	80.9	[41]
Hazelnut shell	38.22	[42]
Straw activated carbon	472.10	[43]
Montmorillonite clay	289.12	[44]
Activated sludge biomass	256.41	[45]
Pomelo (*Citrus grandis*) peel	344.83	[46]

perature on adsorption. The Gibbs free energy change, ΔG, can be determined by the following equation:

$$\Delta G = -RT\ln K'_c \quad (13)$$

$$\Delta G = \Delta H - T\Delta S \quad (14)$$

The apparent equilibrium constant (K'_c) of the adsorption is defined as:

$$K'_C = \frac{C_{ad,e}}{C_e} \quad (15)$$

where $C_{ad,e}$ is the concentration of dyes on the adsorbent at equilibrium (mg/L). The value of K'_c in the lowest experimental NR and MB concentration can be obtained [25]. The K'_c value is used in the Eq. (13) to determine the change of Gibbs free energy (ΔG) of adsorption. Enthalpy change, ΔH, and entropy change, ΔS, were determined from the slope and intercept of the plot according to Eq. (14).

The values of ΔG for NR were −7.48, −9.32, and −10.57 kJ/ mol, and for MB were −6.21, −7.54 and −8.67 kJ/ mol at 283, 298 and 313 K, respectively. The value of ΔH and ΔS for NR was 21.57 and 0.103 kJ/ mol K, and for MB was 16.96 and 0.082 kJ/mol K, respectively.

The positive value of ΔH (endothermic) is indicative of an increase in adsorption on successive increase in temperature. The negative ΔG values indicated thermodynamically feasible and spontaneous nature of the adsorption. The negative value of ΔG decreased with an increase in temperature, indicating that a better adsorption is actually obtained at higher temperatures. The positive value of ΔS reveals the increased randomness at the solid–solution interface during the fixation of NR and MB dyes on the active sites of MPH.

3.7.2. Estimation of activation energy

The magnitude of activation energy may give an idea about the type of sorption. There are two main types of adsorption: physical and chemical. Activated chemical adsorption means that the rate varies with temperature according to a finite activation energy (8.4–83.7 kJ/mol) in the Arrhenius equation. In nonac-

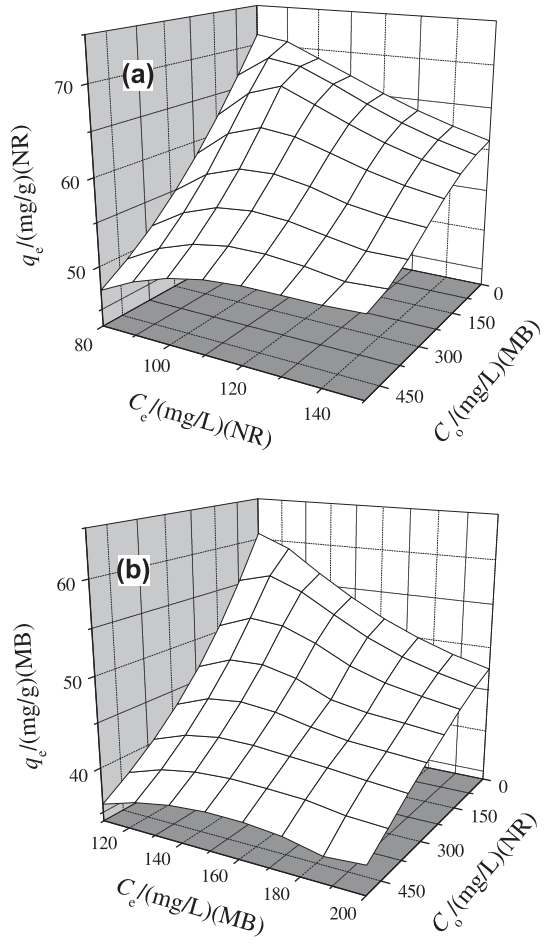

Fig. 8. The binary adsorption isotherm. (a) The adsorption capacity of NR is plotted as a function of the equilibrium concentrations of NR and (b) The adsorption capacity of MB is plotted as a function of the equilibrium concentrations of MB.

tivated chemical adsorption, the activation energy is near zero [25].

The activation energy for NR and MB adsorption was calculated by the Arrhenius equation:

$$k = k_0 e^{-\frac{E_a}{RT}} \tag{16}$$

where k_0 is the temperature independent factor in g/mg min, E_a is the apparent activation energy of the reaction of adsorption in kJ/mol, R is the gas constant, 8.314 J/mol K, and T is the adsorption absolute temperature, K. The linear form is:

$$\ln k = \ln k_0 - \frac{E_a}{RT} \tag{17}$$

When $\ln k$ is plotted vs. $1/T$, a straight line with slope $-E_a/R$ is obtained. The values of rate constant obtained nonlinear analysis according to the pseudo-second order can be used to calculate the activation energy of sorption process. The energy of activation (E_a) was determined from the slope of the Arrhenius plot of $\ln k_2$ vs. $1/T$ (figure not shown) according to Eq. (17) and was found to be 15.25 and 10.24 kJ/mol for NR and MB, respectively. The values were of the same magnitude as the activation energy of activated chemical sorption. The positive values of E_a suggested that rise in temperature favor the adsorption and this may be an endothermic in nature.

3.8. Competitive adsorption of NR and MB in equilibrium

The experiments of competitive adsorption of NR and MB include two parts: (i) the effect on NR adsorption with the presence of MB in the solution, and the effect on MB adsorption with the presence of NR in the solution and (ii) the competitive adsorption of NR and MB in the total concentration did not change.

3.8.1. The effect on adsorption of NR or MB with the presence of MB or NR in the solution

In a series of two binary systems, the initial concentration of NR is fixed to 300 mg/L (1.039 mmol/L), whereas the concentration of MB is varied from 0 to 500 mg/L (0–1.337 mmol/L). In another binary system, the initial concentration of MB is constant at 300 mg/L (0.802 mmol/L) and the concentration of NR is varied from 0 to 500 mg/L (0–1.731 mmol/L). The two (equilibrium) adsorbate concentrations are plotted against the NR or MB uptakes in Fig. 8(a) and (b), respectively.

As shown in Fig. 8, when both NR and MB are present in solution, some reduction of the NR or MB adsorption can be observed with increasing MB or NR concentration. From Fig. 8(a), the interference of MB with the NR adsorption is slightly pronounced. The adsorption capacities q_e of NR decreases from 72.92 to 51.77 mg/g (reduction of 29.0%) in the presence of MB with the initial concentration from 0 to 500 mg/L while the values of q_e of MB decreases from 62.62 to 36.28 mg/g (reduction of 42.1%) in the presence of NR with the concentration from 0 to 500 mg/L. From the extent of quantity reduction, the effect of NR in solution on MB adsorption is stronger. So NR has a better affinity for MPH than MB. This result could be explained by the structure formulas of two dyes. The amino group of NR was bond with benzene ring, but the sulfur of MB was within the

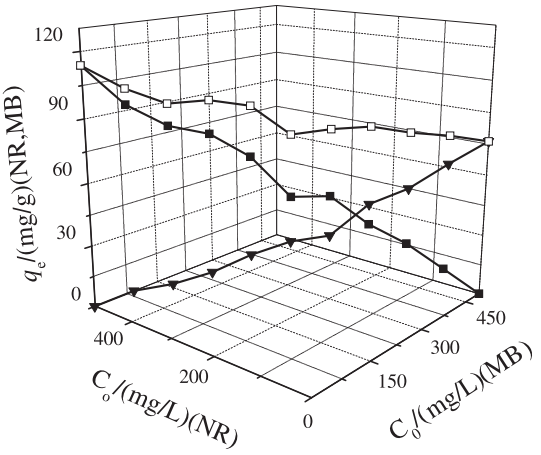

Fig. 9. Effect of the fixed total initial concentration of NR and MB on the adsorption capacity of each adsorbate. (■) q_e (NR) (▼) q_e (MB) (□) q_e (NR)+q_e(MB).

benzene ring. The contact area between MPH and NR would be smaller than that of MPH and MB. In other word, the steric hinderance effect of MB is bigger than that of NR. As a result, MPH would be decrease the biding energy to MB compared to NR when two dyes coexist in solution. So the adsorption capability of NR by MPH was stronger than that of MB. Another reason is that there may be existed hydrogen bond between NH_3^+ (from NR) and COO^- (from adsorbent).

3.8.2. The competitive adsorption of NR and MB at a fixed total concentration

The objective of this part work is to study the effect of NR and MB ions coexistence on the total adsorptive capacity of MPH. The experiment is carried out keeping the total concentration of NR and MB fixed at 500 mg/L and changing each dye concentration. The result is shown in Fig. 9.

As shown in Fig. 9, values of the adsorption capacities q_e obtained from the experiment results for the binary component system at described conditions are less than those for the single component solutions. This indicates that NR in solution can inhibit MB adsorption yield while MB inhibits NR adsorption yield. The data also show that the equilibrium concentration of one adsorbate will be significantly different when the concentration of another adsorbate in solution changes. However, the total adsorption capacity for these two dye ions in the binary system exceeded the capacity of MB but was less than that of NR in the single systems. One type of dye presented in solution interferes with the uptake of another in the same system, and the total adsorbate uptake is lower. In the binary system, there is competitive adsorption between NR ions and MB ions.

3.9. Regeneration

Regeneration of spent adsorbent and recovery of adsorbate would make the treatment process economical. It may decrease the process cost and also the dependency of the process on a continuous adsorbent supply. For this purpose, it is desirable to desorb the adsorbed dyes and to regenerate the adsorbent for another cycle of application. The solution of 0.1 mol/L HCl was tried as renewable adsorbents. The reason may be that there is positively charge on surface of adsorbent. Carbonyl group and hydroxyl group on surface of adsorbent is existed as –COOH and –OH, so the interaction became weak between carbonyl group or hydroxyl group on adsorbent surface and the positive group on the dye molecule. At the first cycle, the solution of 0.1 mol/L HCl performed well with NR and MB removal efficiency around 81.2 and 78.0%, respectively. The second and third cycle showed a decreased efficiency for the eluant. The result showed that 76.5 and 65.6% of adsorbed NR could be recovered back in solution and about 66.8 and 61.7% of the MB adsorbed was desorbed in the second and third adsorption—desorption cycle, respectively. The complex reactions between dye cation ions and MPH may be responsible for the incomplete desorption. The wastage percent of MPH was less than 10% after three adsorption–desorption cycles. Considering the excellent preferential adsorption capacity, small dosage, and low cost, the MPH is still a better choice to remove NR and MB in wastewaters.

4. Conclusion

This study showed that MPH was an excellent sorbent for removal of NR and MB from aqueous solution. The adsorption capacities of NR and MB in single systems are 112.72 ± 10.68 and 99.41 ± 7.12 mg/g, respectively. In binary systems, NR and MB show competitive adsorption and NR exhibit higher affinity and selectivity to MPH. The Langmuir isotherm exhibited a better fit to the MB adsorption data by MPH while the Freundlich isotherm seem to agree better with the NR adsorption. Kinetics data tend to fit well in pseudo-first-order and pseudo-second-order kinetic models. The process mechanism was found to be complex, consisting of both surface adsorption and pore diffusion. The process was spontaneous and endothermic.

Acknowledgments

This work was supported by the Education Department of Henan Province in China (No. 2010A610003)

and Henan Science and Technology Department in China (No. 102102210103).

References

[1] S.T. Akar, A.S. Özcan, T. Akar, A. Özcan, Z. Kaynak, Biosorption of a reactive textile dye from aqueous solutions utilizing an agro-waste, Desalination 249 (2009) 757–761.

[2] C. Xia, Y. Jing, Y. Jia, D. Yue, J. Ma, X. Yin, Adsorption properties of congo red from aqueous solution on modified hectorite: Kinetic and thermodynamic studies, Desalination 265 (2011) 81–87.

[3] E. Bulut, M. Özacar, İ.A. Şengil, Equilibrium and kinetic data and process design for adsorption of Congo Red onto bentonite, J. Hazard. Mater. 154 (2008) 613–622.

[4] I.D. Mall, V.C. Srivastava, N.K. Agarwall, I.M. Mishra, Removal of congo red on coal based mesoporous activated carbon, Dyes Pigments 74 (2007) 34–40.

[5] M.M. Abd El-Latif, Amal M. Ibrahim, Removal of reactive dye from aqueous solutions by adsorption onto activated carbons prepared from oak sawdust, Desalin. Water Treat. 20 (2010) 102–113.

[6] S. Boutemedjet, O. Hamdaoui, Sorption of malachite green by eucalyptus bark as a non- conventional low-cost biosorbent, Desalin. Water Treat. 8 (2009) 201–210.

[7] X.L. Wu, Y. Wang, J.L. Liu, J.Y. Ma, R.P. Han, Study of malachite green adsorption onto natural zeolite in a fixed-bed column, Desalin. Water Treat. 20 (2010) 228–233.

[8] S.T. Ong, E.C. Khoo, S.L. Hii, S.T. Ha, Utilization of sugarcane bagasse for removal of basic dyes from aqueous environment in single and binary systems, Desalin. Water Treat. 20 (2010) 86–95.

[9] R.P. Han, Y.F. Wang, P. Han, J. Shi, J. Yang, Y.S. Lu, Removal of methylene blue from aqueous solution by chaff in batch mode, J. Hazard. Mater. 137 (2006) 550–557.

[10] A.S. Franca, L.S. Oliveira, S.A. Saldanha, P.I.A. Santos, S.S. Salum, Malachite green adsorption by mango (*Mangifera indica* L.) seed husks: Kinetic, equilibrium and thermodynamic studies, Desalin. Water Treat. 19 (2010) 241–248.

[11] V.K. Gupta, Suhas Application of low-cost adsorbents for dye removal—A review, J. Environ. Manage. 90 (2009) 2313–2342.

[12] W.S. Wan Ngah, M.A.K.M. Hanafiah, Removal of heavy metal ions from wastewater by chemically modified plant wastes as adsorbents: A review, Bioresour. Technol. 99 (2008) 3935–3948.

[13] R.M. Gong, S.X. Zhu, D.M. Zhang, J. Chen, S.J. Ni, R. Guan, Adsorption behavior of cationic dyes on citric acid esterifying wheat straw: Kinetic and thermodynamic profile, Desalination 230 (2008) 220–228.

[14] M.M. Abd El-Latif, A.M. Ibrahim, Adsorption, kinetic and equilibrium studies on removal of basic dye from aqueous solutions using hydrolyzed oak sawdust, Desalin. Water Treat. 6 (2009) 252–268.

[15] F. Atmani, A. Bensmaili, A. Amrane, Methyl orange removal from aqueous solutions by natural and treated skin almonds, Desalin. Water Treat. 22 (2010) 174–181.

[16] Z.W. Wang, P. Han, Y. Jiao, D. Ma, C.C. Dou, R.P. Han, Adsorption of congo red using ethylenediamine modified wheat straw, Desalin. Water Treat. 30 (2011) 195–206.

[17] D.W. O'Connell, C. Birkinshaw, T.F. O'Dwyer, Heavy metal adsorbents prepared from the modification of cellulose: A review, Bioresour. Technol. 99 (2008) 6709–6724.

[18] K.S. Low, C.K. Lee, S.M. Mak, Sorption of copper and lead by citric acid modified wood, Wood Sci. Technol. 38 (2004) 629–640.

[19] T. Vaughan, C.W. Seo, W.E. Marshall, Removal of selected metal ions from aqueous solution using modified corncobs, Bioresour. Technol. 78 (2001) 133–139.

[20] P.D. Johnson, M.A. Watsona, J. Browna, I.A. Jefcoat, Peanut hull pellets as a single use sorbent for the capture of Cu(II) from wastewater, Waste Manage. 22 (2002) 471–480.

[21] R.M. Gong, M. Li, C. Yang, Y.Z. Sun, J. Chen, Removal of cationic dyes from aqueous solution by adsorption on peanut hull, J. Hazard. Mater. 12 (2005) 247–250.

[22] L.S. Balistrieri, J.W. Murray, The surface chemistry of goethite (α-FeOOH) in major ion seawater, Am. J. Sci. 281 (1981) 788–806.

[23] W.J. Albrecht, Peanut Hulls: Their properties and potential uses. U.S. Dept of Ag Science and Education Administration, Agricultural Reviews and Manuals, Southern Series, No. 1, 1979.

[24] J.Y. Song, W.H. Zou, Y.Y. Bian, F.Y. Su, R.P. Han, Adsorption characteristics of methylene blue by peanut husk in batch and column modes, Desalination 265 (2011) 119–125.

[25] R.P. Han, L.J. Zhang, C. Song, M.M. Zhang, H.M. Zhu, L.J. Zhang, Characterization of modified wheat straw, kinetic and equilibrium study about copper ion and methylene blue adsorption in batch mode, Carbohyd. Polym. 79 (2010) 1140–1149.

[26] A.K. Meena, G.K. Mishra, P.K. Rai, C. Rajagopal, P.N. Nagar, Removal of heavy metal ions from aqueous solutions using carbon aerogel as an adsorbent, J. Hazard. Mater. 122 (2005) 161–170.

[27] Y.S. Ho, J.C.Y. Ng, G. McKay, Kinetics of pollutant sorption by biosorbents: Review, Sep. Purif. Methods 29 (2000) 189–232.

[28] C.W. Cheung, J.F. Porter, G. Mckay, Sorption kinetics for the removal of copper and zinc from effluents using bone char, Sep. Purif. Technol. 19 (2000) 55–64.

[29] V.C. Srivastava, M.M. Swamy, I.D. Mall, B. Prasad, I.M. Mishra, Adsorptive removal of phenol by bagasse fly ash and activated carbon: Equilibrium, kinetics and thermodynamics, Colloids Surf. A 272 (2006) 89–104.

[30] G.E. Boyd, A.W. Adamson, L.S. Myers Jr., The exchange adsorption of ions from aqueous solutions by organic zeolites. II: Kinetics, J. Am. Chem. Soc. 69 (1947) 2836–2848.

[31] K.K. Singh, R. Rastogi, S.H. Hasan, Removal of Cr(VI) from wastewater using rice bran, J. Colloid Interf. Sci. 290 (2005) 61–68.

[32] I. Langmuir, The constitution and fundamental properties of solids and liquids, J. Am. Chem. Soc. 38 (1916) 2221–2295.

[33] H.M.F. Freundlich, Uber die adsorption in lasungen, J. Phys. Chem. 57 (1906) 385–470.

[34] Q. Zhou, W.Q. Gong, C.X. Xie, D.J. Yang, X.Q. Ling, X. Yuan, S.H. Chen, X.F. Liu, Removal of Neutral Red from aqueous solution by adsorption on spent cottonseed hull substrate, J. Hazard. Mater. 185 (2011) 502–506.

[35] R.M. Gong, X.P. Zhang, H.J. Liu, Y.Z. Sun, B.R. Liu, Uptake of cationic dyes from aqueous solution by biosorption onto granular kohlrabi peel, Bioresour. Technol. 98 (2007) 1319–1323.

[36] W.H. Zou, P. Han, Y.L. Lia, X. Liu, X.T. He, R.P. Han, Equilibrium, kinetic and mechanism study for the adsorption of Neutral Red onto rice husk, Desalin. Water Treat. 12 (2009) 210–218.

[37] D.Y. Yue, Y. Jing, J. Ma, C.Y. Xia, X.J. Yin, Y.Z. Jia, Removal of Neutral Red from aqueous solution by using modified hectorite, Desalination 267 (2011) 9–15.

[38] Q.Q. Shi, J. Zhang, C.L. Zhang, C. Li, B. Zhang, W.W. Hu, J. T. Xu, R. Zhao, Preparation of activated carbon from cattail and its application for dyes removal, J. Environ. Sci. 22 (2010) 91–97.

[39] K.S. Low, C.K. Lee, The removal of cationic dyes using coconut husk as an absorbent, Pertanika 13 (1990) 221–228.

[40] X.S. Wang, Y. Zhou, Y. Jiang, C. Sun, The removal of basic dyes from aqueous solutions using agricultural by-products, J. Hazard. Mater. 157 (2008) 374–385.
[41] R.P. Han, W.H. Zou, W.H. Yu, S.J. Cheng, Y.F. Wang, Jie Shi, Biosorption of methylene blue from aqueous solution by fallen phoenix tree's leaves, J. Hazard. Mater. 141 (2007) 156–162.
[42] M. Dogan, H. Abak, M. Alkan, Biosorption of methylene blue from aqueous solutions by hazelnut shells: Equilibrium, parameters and isotherms, Water Air Soil Pollut. 192 (2008) 141–153.
[43] N. Kannan, M.M. Sundaram, Kinetics and mechanism of removal of methylene blue by adsorption on various carbons—A comparative study, Dyes Pigments 51 (2001) 25–40.
[44] C.A.P. Almeida, N.A. Debacher, A.J. Downs, L. Cottet, C.A.D. Mello, Removal of methylene blue from colored effluents by adsorption on montmorillonite clay, J. Colloid Interf. Sci. 332 (2009) 46–53.
[45] O. Gulnaz, A. Kaya, F. Matyar, B. Arikan, Sorption of basic dyes from aqueous solution by activated sludge, J. Hazard. Mater. B108 (2004) 183–188.
[46] B.H. Hameed, D.K. Mahmoud, A.L. Ahmad, Sorption of basic dye from aqueous solution by pomelo (*Citrus grandis*) peel in a batch system, Colloids Surf. A316 (2008) 78–84.

Appendix

The structure of Methylene blue (MB, C.I.52015, FW = 373.9) and Neutral Red (NR, C.I.50040, FW = 288.8) are as following:

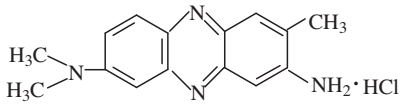

NR

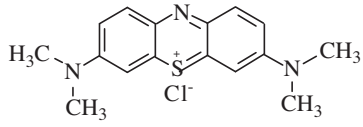

MB